Geophysical Prospecting **36**, 614–632, 1988

THE EFFECT OF THE ASPECT RATIO ON CRACK-INDUCED ANISOTROPY[1]

J. DOUMA[2]

ABSTRACT

DOUMA, J. The effect of the aspect ratio on crack-induced anisotropy. *Geophysical Prospecting* **36**, 614–632.

Media containing aligned cracks show anisotropy with respect to elastic wave propagation. There are several models describing the wave propagation in cracked media, most of them only valid for cracks with small aspect ratios. One of these models (Crampin's model) is compared with a model valid for all aspect ratios (Nishizawa's model). The elastic constants and the group velocities are compared for both dry and liquid-filled inclusions with aspect ratios ranging from 0.0001 (flat cracks) up to 1 (spheres). The difference between both models is small for small aspect ratios but becomes larger for increasing aspect ratios. At a crack density of 0.05 both models give–within an error of 5%—the same results for aspect ratios up to 0.3. Therefore Crampin's model can be applied to a large range of cracked media even if the aspect ratio of the inclusions is not small. The variation of the anisotropy as a function of the aspect ratio can be studied using Thomsen's dimensionless parameters δ, ε and γ. They show how inclusions with large aspect ratios result in elliptical anisotropy.

INTRODUCTION

Anisotropy with respect to elastic wave propagation is becoming important in geophysical research nowadays. Seismic anisotropy was studied more than 30 years ago (Postma 1955; Helbig 1956, 1958), but for a long time its effect was considered to be negligible. Helbig (1984) pointed out this was because most of the seismic data recorded were P-wave reflection data obtained for P-waves travelling at small angles to the vertical axis of the medium. In a transversely isotropic medium with a vertical axis of symmetry (e.g. caused by thin horizontal layering), such P-waves (and thus most of the reflection seismic surveys) would only be slightly affected (Krey and Helbig 1956). This is the main reason why most seismic surveys could be carried out without considering the effect of anisotropy. However, for special acquisition geometries (like Vertical Seismic Profiling (VSP)) where large angles of incidence may occur, the effect of anisotropy has to be taken into account (Uhrig and Van Melle 1955).

[1] Received September 1987, accepted January 1988.

[2] Department of Exploration Geophysics, Institute for Earth Sciences, P.O. Box 80 021, 3508 TA Utrecht, The Netherlands.

During the last few years it has been realized that anisotropy can play an important role in seismic exploration. This is primarily due to the increasing use of shear waves, which are much more sensitive to anisotropy than P-waves (Crampin, Chesnokov and Hipkin 1984). Without taking anisotropy into account it is often difficult to interpret shear-wave data (Alford 1986). Secondly, it is due to the quantity of information that can be derived from shear waves showing anisotropy effects. (Crampin (1985) claims that there is at least 3 times as much information in shear waves than in P-waves.) Crampin shows in many papers how shear-wave splitting can be used to find the orientation and crack density of aligned circular cracks. Because these cracks may exist in hydrocarbon reservoirs this information may be of great importance in evaluating these reservoirs (Crampin 1987). Cracks are also assumed to play an important role in earthquake prediction (Crampin, Evans and Atkinson 1984). It is believed that the geometry of cracks will change due to variations in the stress field just before an earthquake takes place. Consequently, the anisotropy may also change. If temporal changes in this anisotropy could be observed, it might be possible to monitor the build up of stress preceding an earthquake.

Recently anisotropy effects have been observed in seismic data and have been attributed to aligned cracks, although many other possible causes of anisotropy (e.g. thin layering, aligned crystals, aligned grains, etc.) may exist (Crampin 1987). This could only be justified after theoretical models describing the wave propagation in cracked media had been developed and the results compared with experimental data. It turned out that many of the anisotropy effects observed in the Earth's crust could be modelled by cracked media. In the comparison of modelled and real data, hodograms and velocity variation diagrams were used. From the best fit the parameters describing the cracks (e.g. crack density, aspect ratio, and the orientation of the cracks) were estimated (Crampin, McGonigle and Bamford 1980; Crampin, McGonigle and Ando 1986)

However, a number of problems has to be solved before an inversion for these parameters will have a high level of confidence. Some of these problems were pointed out at the workshop on anisotropy held at the 49th EAEG meeting in Belgrade, 1987. The papers presented at this workshop will be published in a special issue of *Geophysical Transactions*, Eötvös Loránd Geophysical Institute of Hungary.) There are, for example, serious practical problems with respect to the construction of reliable hodograms from three-component VSP measurements and problems as to whether the two shear waves travel along the same raypath (as assumed in many anisotropy analyses). Moreover, it is even possible to have polarization effects in isotropic media that might be misinterpreted as anisotropy effects (Douma and Helbig 1987).

Apart from these problems which may complicate the estimation of the crack parameters from experimental data, the theory used to describe the wave propagation in cracked media is also critical. Different theories may result in different crack parameters describing the same data. Therefore, it is important to know the limitations of each theory. We here investigate a theory valid for all aspect ratios of the cracks and compare it with one often used to describe the wave propagation in cracked media, but only valid for small aspect ratios.

Flat Crack Models

Several theories have been developed to calculate the effective elastic constants of media containing aligned circular cracks. They all assume that the dimensions of the cracks are small with respect to the seismic wavelengths used. The theories that have often been used in geophysics are due to Garbin and Knopoff (1973, 1975a, b) and Hudson (1980, 1981). They are all based on the scattering of waves at the cracks. These theories have been used (Crampin 1978, 1984; Crampin *et al.* 1980, 1986) to analyse wave propagation in cracked media and to explain observed anisotropy. The basic assumptions of these theories are that the cracks are in dilute concentration and have small aspect ratios.

A theory that is valid for large concentrations of cracks has been proposed recently by Thomsen (1988) and is based on the work of Hoenig (1979), who calculated the elastic constants of a cracked medium using a self-consistent approach. In such an approach the interactions between the cracks are taken into account by estimating the behaviour of a single crack in the composite medium as that of a single crack in the equivalent homogeneous medium. Although Hoenig's model is not restricted by the assumption of a dilute concentration of cracks, it does assume a small aspect ratio of the cracks, just like the other models mentioned. Therefore we call them 'flat crack models'. (Thomsen (1988) has compared some of these models.) In a review on rock physics Yale (1985) considers the assumption of small aspect ratios a serious drawback of these models, which should not exist in future models. Apparently, Yale (1985) was unaware of theories that do model large aspect ratios correctly.

Ellipsoidal Inclusion Models

Anderson, Minster and Cole (1974) and Nishizawa (1982) presented models that calculate the effective elastic constants of media containing aligned ellipsoidal inclusions. (Note that there are some misprints in Nishizawa's paper (1982): to use the equations for $\bar{G}_{ijkl}$ in the appendix (9) should be divided by 8π, the term 4π in (10) should be omitted and note that $\bar{G}_{ijkl} = \bar{G}_{jikl} = \bar{G}_{ijlk}$.) A small size of the inclusions with respect to the wavelengths used is assumed. The ellipsoids have two equal semi-axes a, whereas the third axis (the axis of rotational symmetry) may have any length b. The ratio b/a is called the aspect ratio. Circular cracks are one limiting case of these ellipsoids for very small aspect ratios ($b/a \to 0$). Unlike the flat crack models, Anderson's and Nishizawa's models are valid for all aspect ratios.

We will include a short review of both models. They are based on the results obtained by Eshelby (1957). Eshelby suggested a static approach to calculate the effective elastic constants of a medium containing aligned ellipsoidal inclusions. His approach is based on two hypothetical processes:

(1) introducing the inclusions keeping the surface tractions constant, and
(2) introducing the inclusions keeping the surface displacements constant.

From the change in elastic energy of the medium due to these processes the elastic constants can be found. To avoid interactions between the inclusions their concentration has to be dilute.

Anderson's model is based on Eshelby's second process of keeping the surface displacements constant. Nishizawa (1982) pointed out that Anderson would have obtained different results by using the first process. To avoid this discrepancy Nishizawa developed a numerical algorithm which can calculate the effective elastic constants even for large concentrations of ellipsoids. Considering a volume concentration of ellipsoids embedded in a homogeneous background material he first calculated the effective elastic constants of the background material containing only a small portion of ellipsoids (in order to use Eshelby's equations which are only valid for dilute concentrations of ellipsoids). Then a small portion of the remaining concentration of ellipsoids was added to the resultant anisotropic medium calculated in the first step and the effective constants were calculated again. This process was repeated until the effect of the total concentration of inclusions has been calculated.

We compare Nishizawa's method with Hudson's flat crack model (Hudson 1980, 1981). Hudson's model (valid for first- and second-order perturbations in the crack density) became well known because Crampin (e.g. Crampin 1984, 1985) has often used it and we will refer to this specific model as 'Crampin's model'. The purpose of a comparison between Nishizawa's and Crampin's models is to obtain the aspect ratios for which both models result in the same anisotropy. This will indicate the range of aspect ratios for which Crampin's flat crack model is valid. The need to know this range becomes clear when velocity variations in cracked media are studied for different aspect ratios using Crampin's model, although it is realized that the results may be suspect for large aspect ratios (Crampin *et al.* 1986). When it is known for what range of aspect ratios Crampin's model is valid, it can be judged whether the results of these studies should be corrected or not.

Further, Nishizawa's model is carefully studied to gain a better understanding of the role the aspect ratio of the cracks plays in the resultant anisotropy of cracked media. Although Crampin (1987, Table 2) shows that there are many parameters influencing the anisotropy, the aspect ratio is probably one of the most important (Crampin 1987).

Wave Propagation in Cracked Media

A medium containing aligned circular cracks or aligned ellipsoidal inclusions can be replaced by a homogeneous transversely isotropic medium. Transverse isotropy is a special case of anisotropy and is described by five independent elastic constants, whereas anisotropy in general is described by up to 21 independent constants. Media having an axis of rotational symmetry which may be oriented in any direction show transverse isotropy. If this axis is not vertical this type of anisotropy is sometimes called 'azimuthal anisotropy' (Crampin 1986).

Once the effective elastic constants of such a medium are known (e.g. when they have been calculated with one of the theoretical models described earlier) the characteristics of wave propagation through this medium can be modelled. Many such studies have been carried out (Helbig 1958; Keith and Crampin 1977a, b, c; Crampin 1981). We will summarize their main features.

In anisotropic media there are three body waves in every direction of phase propagation with mutually orthogonal displacements. In general, none of the waves has a polarization parallel (longitudinal direction) or perpendicular (transverse direction) to the wave normal. For weak anisotropy, however, the polarization of the waves is close to these directions and, therefore, there are a quasi-longitudinal wave (qP-wave) and two quasi-transverse waves (qS_1- and qS_2-wave). In any symmetry plane of the medium the polarization of the qP-wave and one of the quasi-transverse waves (called qSP) are parallel to this plane whereas the other quasi-transverse wave (called qSR) is polarized perpendicular to the plane. qP-, qSP- and qSR-waves are studied in this paper.

All three waves have different velocities which depend on the angle between the wave normal and the symmetry axis of the medium. Two velocities can be used to describe wave propagation in anisotropic media: the phase velocity normal to the wavefront, and the group velocity—the velocity of energy propagation. The exact formulae relating these quantities to the elastic constants can be found in the references mentioned above.

The exact formulae for transverse isotropy contain five independent elastic parameters. This number can be reduced to four by using dimensionless parameters. In recent studies (Thomsen 1986) approximate formulae were derived for weak transverse isotropy containing only three dimensionless parameters. These formulae give the linearized phase velocities $v(\theta)$:

$$v_{qP}(\theta) \approx v_P(1 + \delta \sin^2 \theta \cos^2 \theta + \varepsilon \sin^4 \theta), \tag{1a}$$

$$v_{qSP}(\theta) \approx v_S\left(1 + \frac{v_P^2}{v_S^2}(\varepsilon - \delta) \sin^2 \theta \cos^2 \theta\right), \tag{1b}$$

$$v_{qSR}(\theta) \approx v_S(1 + \gamma \sin^2 \theta), \tag{1c}$$

where $v_P = \sqrt{(C_{33}/\rho_e)}$ and $v_S = \sqrt{(C_{44}/\rho_e)}$ are the velocities along the symmetry axis (assumed to be directed along the x_3 axis), ρ_e is the density of the effective medium, θ the angle between the wave normal and the symmetry axis, and C_{33} and C_{44} are elements of the elastic tensor denoted compactly according to the Voigt nomenclature (see e.g. Thomsen 1986).

The anisotropy parameters δ, ε and γ are combinations of elastic constants:

$$\delta = \frac{(C_{13} + C_{44})^2 - (C_{33} - C_{44})^2}{2C_{33}(C_{33} - C_{44})}, \tag{2a}$$

$$\varepsilon = \frac{C_{11} - C_{33}}{2C_{33}}, \tag{2b}$$

$$\gamma = \frac{C_{66} - C_{44}}{2C_{44}}. \tag{2c}$$

As stated by Thomsen (1986) there is no reason to use these linearized expressions for computational purposes but they are useful because their simplicity aids in the understanding of the effect of anisotropy. The parameters are all zero for isotropic media and their deviation from zero can be regarded as a degree of anisotropy. The parameters δ, ε and γ are easy to derive and interpret.

Equations (1a)–(1c) show that the parameter ε represents the relative difference between the qP-phase velocities perpendicular and parallel to the axis of symmetry:

$$\varepsilon \approx \frac{v_{qP}(\pi/2) - v_P}{v_P}. \tag{3a}$$

γ represents this difference for the qSR-waves:

$$\gamma \approx \frac{v_{qSR}(\pi/2) - v_S}{v_S}. \tag{3b}$$

Finally, the parameter δ is

$$\delta \approx 4\left(\frac{v_{qP}(\pi/4)}{v_{qP}(0)} - 1\right) - \left(\frac{v_{qP}(\pi/2)}{v_{qP}(0)} - 1\right) \tag{3c}$$

and can thus be obtained from measurements at $\theta = 0°$, 45° and 90°. Because the parameters δ, ε and γ can easily be estimated from real data the modelling of observed weak anisotropy is simpler with (1a)–(1c) than with most of the other (exact) formulae for phase velocities which need estimates of the elastic constants.

As shown by Thomsen (1986), δ, ε and γ are <0.2 for weak-to-moderate anisotropy. Furthermore, as shown by (2a), δ dominates most anisotropy effects at small angles θ for qP-waves (unless $\varepsilon \gg \delta$), whereas ε does this at θ close to $\pi/2$.

Finally, Thomsen (1986) states that elliptical anisotropy will be observed if δ equals ε. Rudzki (1911) showed that such a type of anisotropy implies ellipsoidal qP-wavefronts while the qSP-wavefronts become spherical. Berryman (1979) and Helbig (1979) showed that elliptical anisotropy can never be caused by thin-layered isotropic media. The significance of elliptical anisotropy in exploration geophysics has been discussed by Helbig (1983).

Because the parameters δ, ε and γ are easily interpretable and give a comprehensive view on anisotropy we used them to model and study the variation of the anisotropy as a function of the aspect ratio.

Numerical Results and Discussion

We compare Nishizawa's ellipsoid model with Crampin's flat crack model. Nishizawa's model is also studied in terms of the parameters δ, ε and γ.

The comparison is carried out for dry and liquid-filled inclusions. Both types of inclusions are investigated because they have often been used to model experimental data (e.g. Crampin *et al.* 1986). The dry inclusions have Lamé constants

$\lambda_1 = \mu_1 = 0$, whereas the liquid-filled inclusions have Lamé constants $\lambda_1 = 15$ kbar and $\mu_1 = 0$. The isotropic background material is the same as used by Crampin (1984), i.e. its density $\rho_b = 2.6$ g cm^{-3} and its Lamé constants are $\lambda_2 = 291.4$ kbar and $\mu_2 = 291.6$ kbar (corresponding to a P-wave velocity of 5.8 km s^{-1} and an S-wave velocity of 3.349 km s^{-1}). Different crack densities e are studied. Two possible expressions for the crack density are

$$e = Na^3/V \tag{4}$$

and

$$e = 3\phi/4\pi\alpha, \tag{5}$$

where N is the number of cracks of radius a in a volume V, ϕ the total volume of the inclusions, and α their aspect ratio.

Comparison of elastic constants

First the resultant elastic constants calculated with Nishizawa's and Crampin's models are compared (a similar comparison between Nishizawa's model and a joint model was carried out by Schoenberg and Douma (1988)). We define their normalized 'Euclidean distance' D as the root mean square of the normalized differences between the five independent elastic constants calculated with Nishizawa's model (C_{11}^N, C_{13}^N, C_{33}^N, C_{44}^N, C_{66}^N) and Crampin's model (C_{11}^C, C_{13}^C, C_{33}^C, C_{44}^C, C_{66}^C). The normalization is carried out with the elastic constants of the background material (C_{11}^b, C_{13}^b, C_{33}^b, C_{44}^b, C_{66}^b):

$$D = \left(\frac{\left(\frac{C_{11}^N - C_{11}^C}{C_{11}^b}\right)^2 + \left(\frac{C_{13}^N - C_{13}^C}{C_{13}^b}\right)^2 + \left(\frac{C_{33}^N - C_{33}^C}{C_{33}^b}\right)^2 + \left(\frac{C_{44}^N - C_{44}^C}{C_{44}^b}\right)^2 + \left(\frac{C_{66}^N - C_{66}^C}{C_{66}^b}\right)^2}{5} \right)^{1/2} \tag{6}$$

In Fig. 1 the distance D is calculated for three crack densities, $e = 0.001$, 0.01 and 0.05 for aspect ratios ranging from $\alpha = 0.0001$ (almost flat cracks) up to $\alpha = 1$ (spheres). In Fig. 1a the result is shown for dry inclusions and in Fig. 1b for liquid-filled inclusions. Both figures show that the distance D is small for small aspect ratios but increases for increasing aspect ratio. Moreover, D increases for increasing crack density. If we consider $D = 0.05$ to be the upper limit for which Crampin's and Nishizawa's model give similar results, both Figs 1a and 1b show that this limit is reached at aspect ratios around $\alpha = 0.3$ for a crack density $e = 0.05$. It is clear from both figures that the distance is not sensitive to the type of inclusion. Thus, for a large range of aspect ratios both models give the same results. We will call this range of aspect ratios the 'crack range'. This crack range is large for small crack densities, but becomes smaller for increasing crack densities.

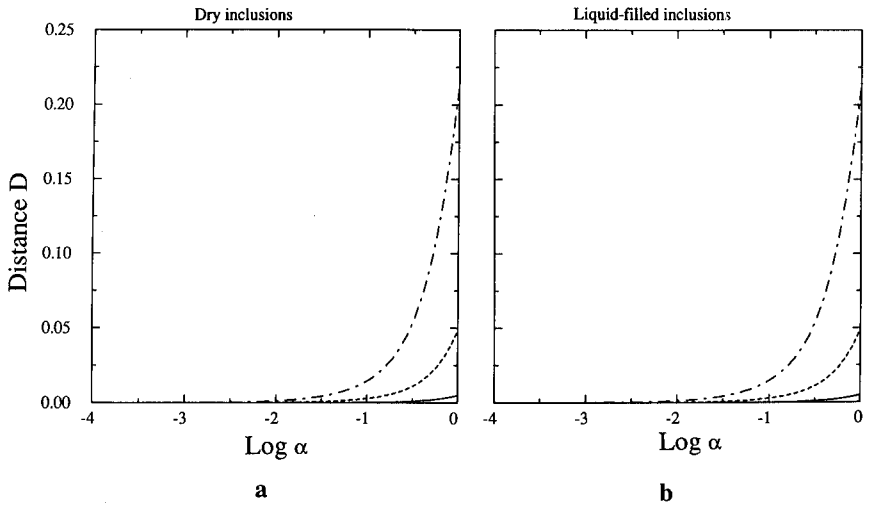

FIG. 1. Normalized distance D between Nishizawa's and Crampin's model as a function of the aspect ratio α of (a) dry inclusions and (b) liquid-filled inclusions embedded in an isotropic background medium. The results are shown for three crack densities $e = 0.001$ (——), $e = 0.01$ (— — —) and $e = 0.05$ (· — · — ·).

Comparison of the group velocities

Although the comparison of elastic constants shown in Figs 1a and 1b gives insight into the differences between Crampin's and Nishizawa's model, it is also instructive to compare the velocities resulting from both models. Modelled velocities (either phase or group velocities) are often used to explain observed velocity variations in real data, and therefore, it is important to know how large the difference is between the velocities calculated with both models and at what angles this occurs. The velocity studied here is the group velocity, because this is the velocity of energy transport which is generally calculated from the arrival times of body waves.

To calculate the velocity not only the elastic contants of the effective medium need to be known but its density ρ_e as well. If the total porosity ϕ of the inclusions is small this density can be closely approximated by the density ρ_b of the background material (i.e. $\rho_e = \rho_b = 2.6$ g cm^{-3}). However, for large porosities the density of the effective medium changes if the density of the inclusions is different from that of the background. Changes in the effective density should be taken into account in the calculation of the velocities. However, to study only the influence of the aspect ratio on the velocity we will first assume a constant effective density ($\rho_e =$ 2.6 g cm^{-3}).

Consider the liquid-filled inclusions embedded in the isotropic background medium. Let the crack density $e = 0.05$. In Figs 2a–c the resultant group velocities of the qP-, qSP- and qSR-waves calculated with Crampin's model are shown, respectively, as a function of the angle against the symmetry axis. Figures 2d–f show the same for Nishizawa's model. In each figure the group velocity is calculated for

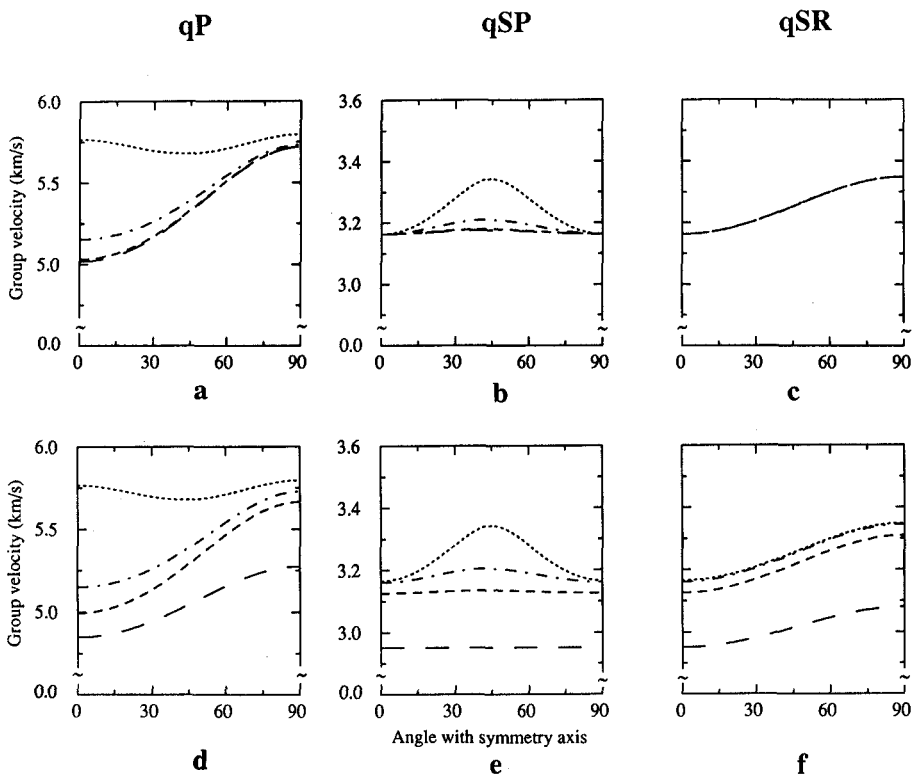

FIG. 2. The group velocity of the qP- (a, d), qSP- (b, e) and qSR-waves (c, f) travelling through an isotropic medium containing liquid-filled inclusions as a function of the angle (in degrees) between the ray direction and the symmetry axis of the effective medium. The upper figures (a, b and c) are calculated with Crampin's model and lower ones (d, e and f) with Nishizawa's model. Four aspect ratios of the inclusions are considered: $\alpha = 0.0001$ (·····), $\alpha = 0.01$ (·-·-·), $\alpha = 0.1$ (----) and $\alpha = 0.5$ (———). The crack density of the inclusions is $e = 0.05$.

four aspect ratios, i.e. $\alpha = 0.0001$, 0.01, 0.1 and 0.5. Comparing the upper and lower figures it can be seen that both models give almost the same results for the small aspect ratios $\alpha = 0.0001$ and $\alpha = 0.01$. However, for the two larger aspect ratios $\alpha = 0.1$ and $\alpha = 0.5$, there is an increasing difference between the results of both models. In spite of this difference the variation of the group velocities as a function of the ray direction does not change much for increasing aspect ratios. This seems to confirm Crampin's assumption that the overall pattern of the velocity variations for large aspect ratios would be similar to that for small aspect ratios, although the exact values may be different (Crampin *et al.* 1986).

Figures 2d–f also show that an increasing aspect ratio tends to reduce the group velocity. Nishizawa's model shows that this is even true for the qSR-waves, which do not show a dependence on the aspect ratio for Crampin's model.

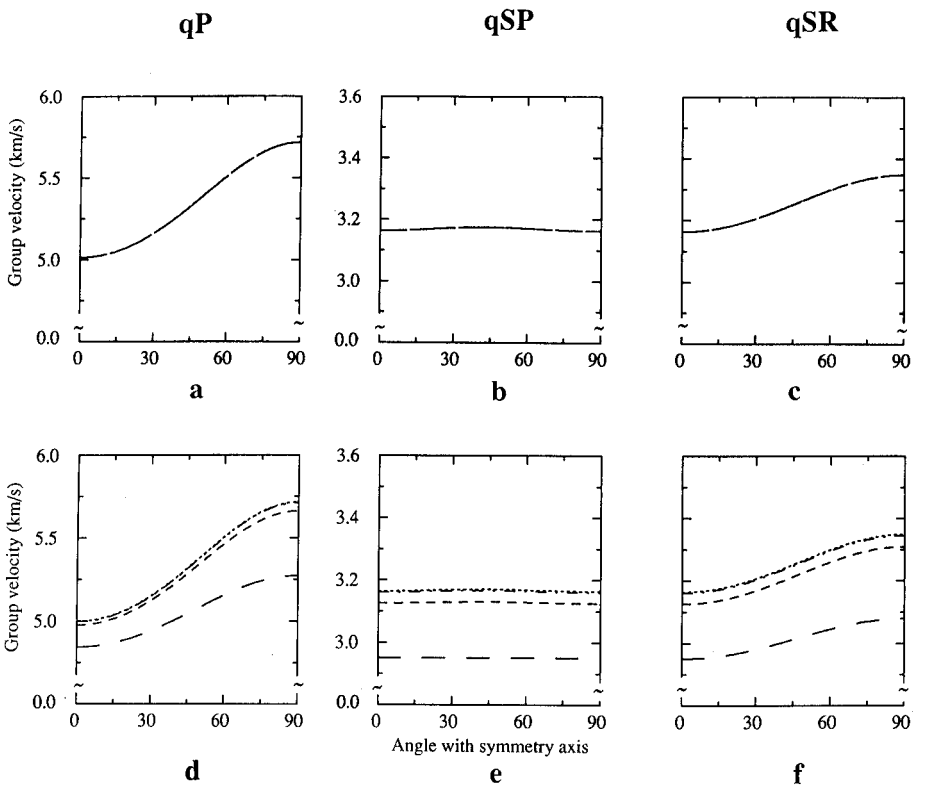

FIG. 3. As in Fig. 2, but for dry inclusions.

The same calculations have been carried out for dry inclusions. The results are shown in Fig. 3, which confirms the conclusions drawn from Fig. 2: both models give almost the same results for small aspect ratios, whereas a difference between the results arises for large aspect ratios. Note, however, that for Crampin's model none of the waves (qP, qSP and qSR) shows a dependence of the group velocity on the aspect ratio, whereas for Nishizawa's model such a dependence exists for each of them.

The velocities of the media studied here are typical for basement forming material. Calculations carried out for sedimentary rocks (but not shown here) give the same similarities and differences between both models as observed in this section.

Normalized difference between group velocities

To study the exact values of the differences in group velocity between both models we calculated, for each wave (qP, qSP and qSR), the normalized difference $D_{NC}(\theta)$,

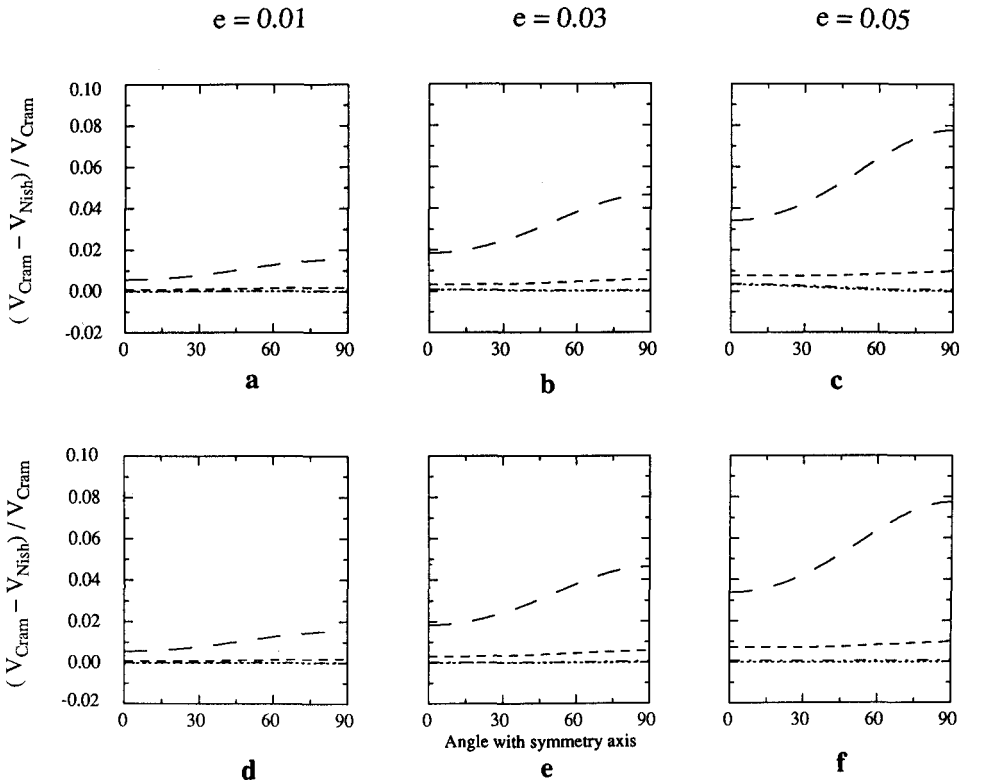

FIG. 4. Normalized difference between the qP-group velocities calculated with Crampin's and Nishizawa's model as a function of the ray direction. Three crack densities are studied: $e = 0.01$ (a and d), $e = 0.03$ (b and e) and $e = 0.05$ (c and f). Figures a, b and c show the results for dry inclusions and figures d, e and f for liquid-filled inclusions.

defined as

$$D_{NC}(\theta) = \frac{(v_{Cram}(\theta) - v_{Nish}(\theta))}{v_{Cram}(\theta)}, \tag{7}$$

where $v_{Cram}(\theta)$ and $v_{Nish}(\theta)$ denote the group velocities calculated with Crampin's and Nishizawa's models, respectively. This was done for three different crack densities $e = 0.01$, 0.03 and 0.05 for both dry and liquid-filled inclusions. In Fig. 4 the results are shown for the qP-wave. The upper Figs 4a–c, are calculated for the dry inclusions and the lower Figs 4d–f, for the liquid-filled inclusions. Figures 4a–f show that there is hardly any difference between the results when either dry or liquid-filled inclusions are studied. They also show more quantitatively than Figs 2 and 3 that the difference between Crampin's and Nishizawa's model is almost zero for small aspect ratios but increases for larger aspect ratios. The differences increase for increasing crack density and angle of incidence. In general, most of the differences are smaller than 0.05 indicating that for most of the crack parameters studied there is a

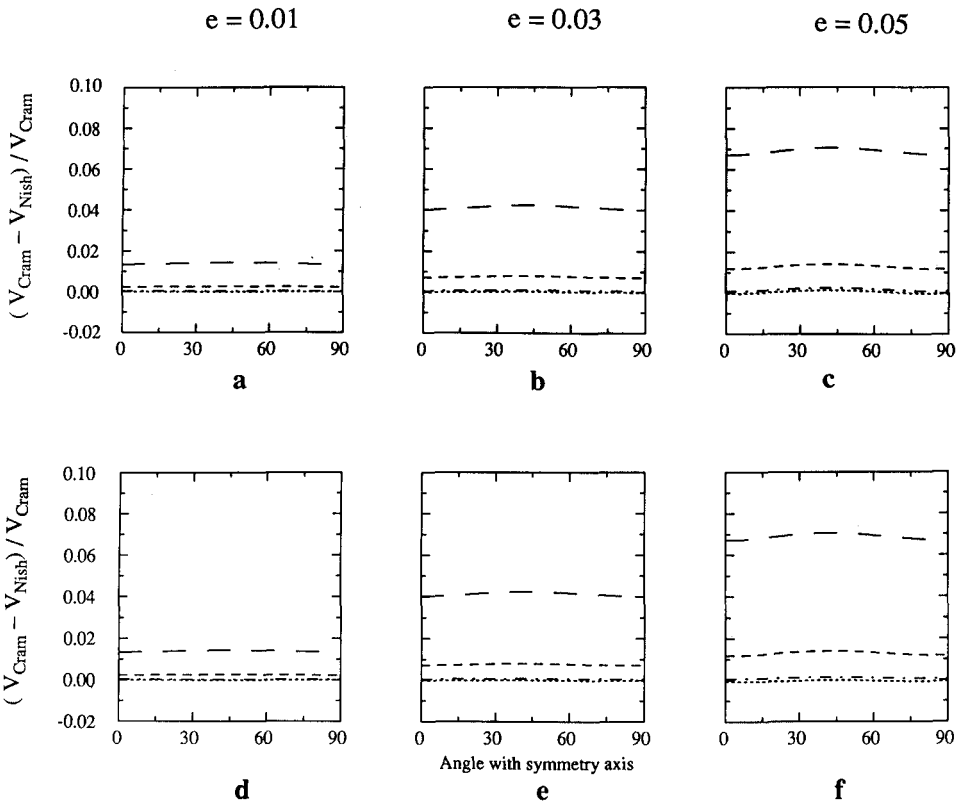

FIG. 5. As in Fig. 4, but for the qSP-group velocity.

good correspondence between the two models. Only for large aspect ratios α and large crack densities e (e.g. $\alpha = 0.5$ and $e = 0.05$) does this correspondence start to fail.

The same calculations have been carried out for qSP- (Fig. 5) and qSR-waves (Fig. 6). They all show the same characteristics as for the qP-waves (Fig. 4), except that qSP-waves always have a maximum difference at $\theta = 45°$, whereas qP- and qSR-waves have such a maximum at $\theta = 90°$.

The influence of the effective density on the group velocity

The results of Figs 4–6 are not influenced by a change in the density ρ_e of the effective medium, because the ratio $D_{NC}(\theta)$ does not depend on the density ρ_e. However, Figs 2 and 3 would be influenced by such a change. In these figures the density was assumed constant to isolate the effect of the aspect ratio on the group velocity. Therefore, the magnitudes of the velocities shown may be in error. The correct value of the effective density is

$$\rho_e = (1 - \phi)\rho_b + \phi\rho_i, \tag{8}$$

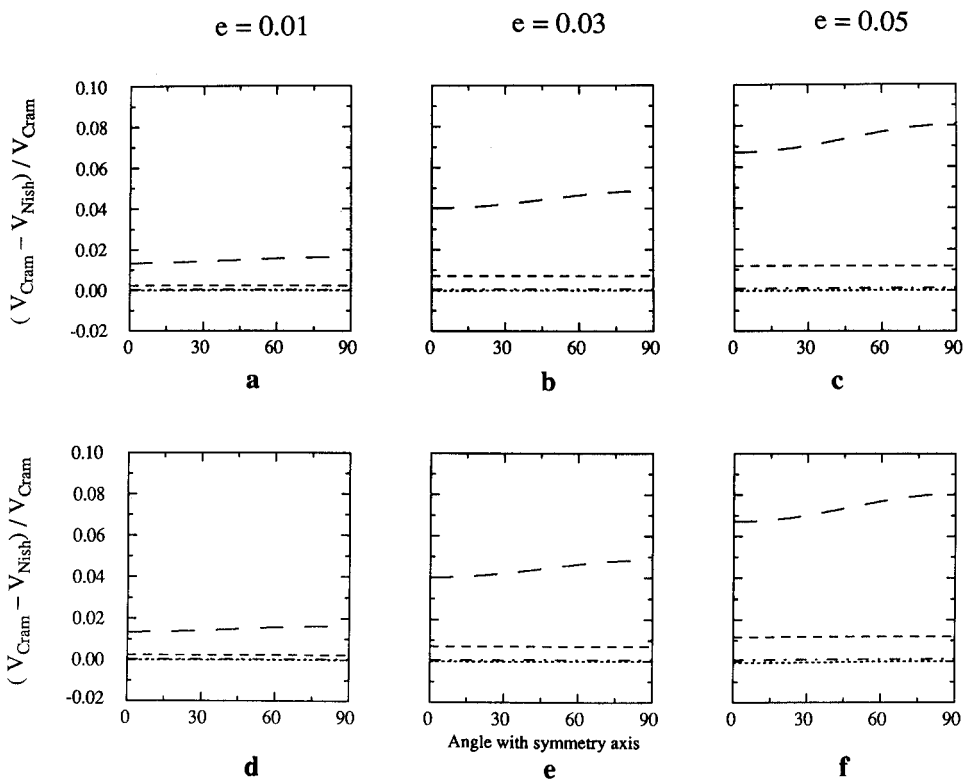

FIG. 6. As in Fig. 4, but for the qSR-group velocity.

where ρ_e, ρ_b, and ρ_i are the densities of the effective medium, background material, and the inclusion material, respectively, and ϕ is the volume concentration of the inclusions.

To study the effect of the density on the group velocities we calculated these velocities for our background medium containing liquid-filled and dry inclusions. The results are presented in Figs 7 and 8, respectively. Figures 7a–c and 8a–c show the group velocities assuming a constant density ρ_e, whereas Figs 7d–f and 8d–f show the results for the correct density ρ_e (calculated with (8)). The densities ρ_i of the liquid-filled and dry inclusions were $\rho_i = 0.93$ g cm^{-3}, and $\rho_i = 0$, respectively. In both sets of figures the velocities were studied for four different aspect ratios $\alpha = 0.0001$, 0.1, 0.5, and 1 (i.e. the inclusions range from flat cracks to spheres). The crack density of the inclusions was $e = 0.05$.

A comparison between the results obtained for the correct density ρ_e with those calculated for a constant density ρ_e shows that the velocities increase when the correct density is taken into account. This effect is negligible for small aspect ratios but becomes strong for large aspect ratios.

Such a phenomenon can be explained by a reduction in the effective density ρ_e. That this reduction is zero for small aspect ratios but becomes significant for larger

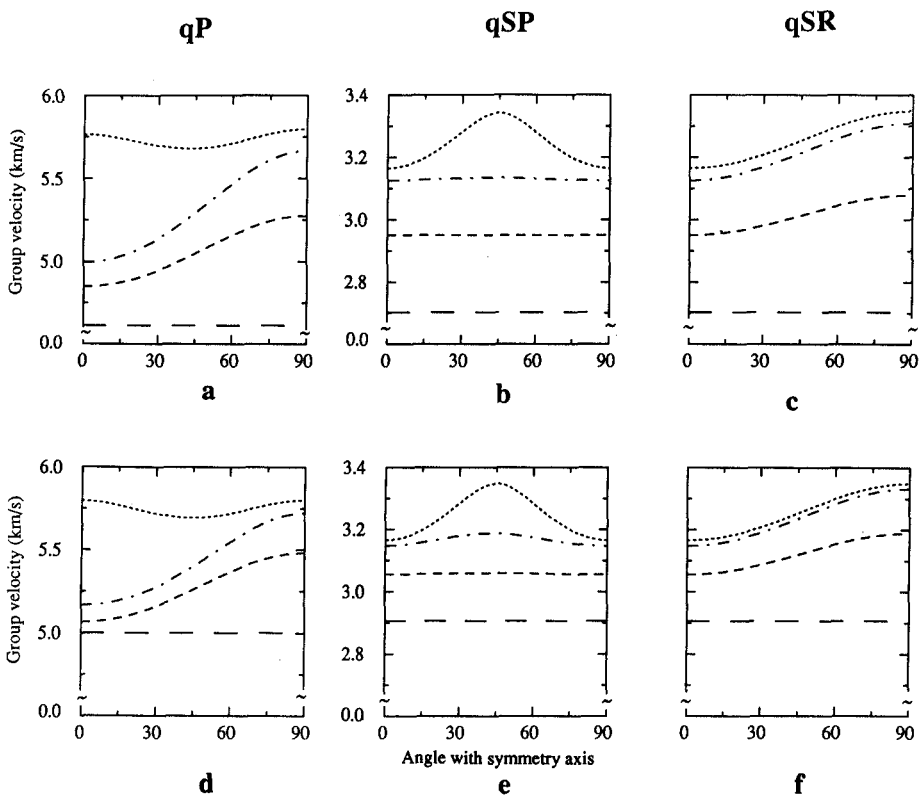

FIG. 7. The group velocities of the qP- (a and d), qSP- (b and e) and qSR-waves (c and f) travelling through an isotropic medium containing liquid-filled inclusions as a function of the ray direction. The results are calculated with Nishizawa's model using a constant density of the effective medium (a, b and c) and using the correct density (d, e and f). Four aspect ratios are considered: $\alpha = 0.0001$ (·····), $\alpha = 0.1$ (·–·–·), $\alpha = 0.5$ (– – – –) and $\alpha = 1$ (————). The crack density of the inclusion is $e = 0.05$.

aspect ratios is clear from (8), which shows that ρ_e starts to deviate from ρ_b for increasing inclusion porosity ϕ. This is only true if $\rho_i \neq \rho_b$ (with significant difference) as in our situation. At a constant crack density an increasing porosity can only be obtained if the aspect ratio increases (see (5)).

From Figs 2 and 3, calculated at a constant density $\rho_e = \rho_b$, we concluded that the group velocities were reduced by an increasing aspect ratio. From Figs 7 and 8 we now conclude that a large part of this reduction vanishes due to the decreasing value of the effective density ρ_e for larger aspect ratios. As might be expected, this density ρ_e has the strongest effect on the results of dry cracks (Fig. 8), because then the density of the inclusion material ($\rho_i = 0$) differs most from the density of the background medium.

Both Figs 7 and 8 show that the effective medium is isotropic when the inclusions are spherical ($\alpha = 1$). The velocities no longer depend on the ray direction and

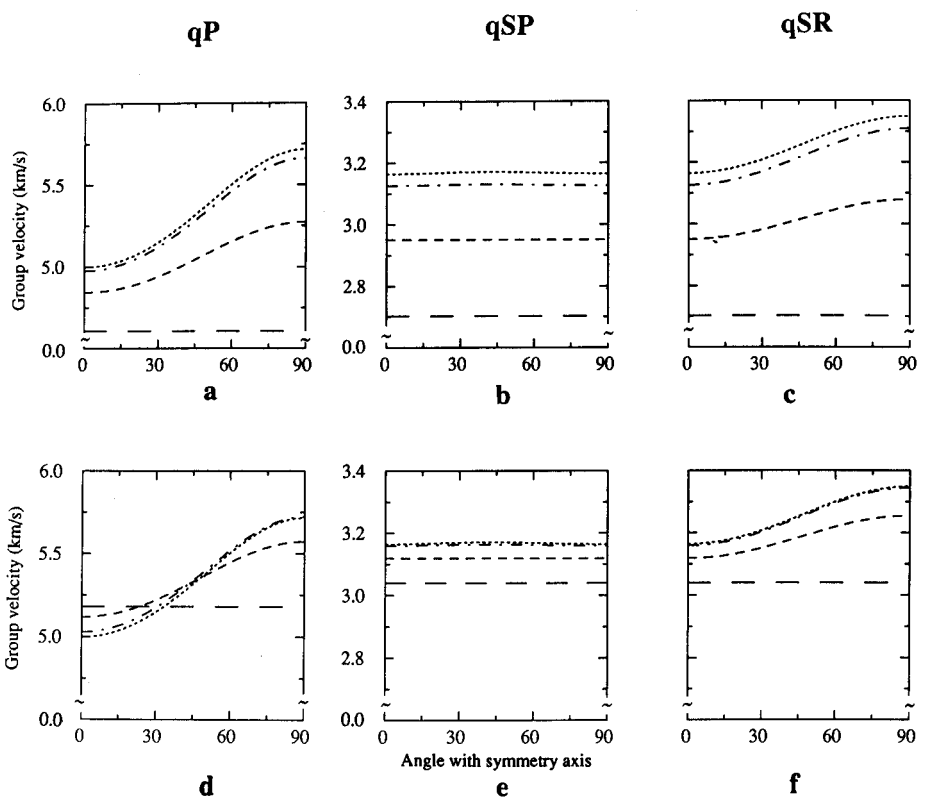

FIG. 8. As in Fig. 7, but for dry inclusions.

there are only two different velocities: the velocity of the qP-waves and the velocity of the qSP-wave, which is equal to that of the qSR-wave.

Anisotropy analysis using the parameters δ, ε and γ

At the end of this section on numerical results we evaluate the anisotropy due to aligned ellipsoidal inclusions by calculating Thomsen's parameters δ, ε and γ. Nishizawa's model is used to calculate the elastic constants. Figure 9 shows the results for dry (Figs 9a and 9b) and liquid-filled inclusions (Figs 9c and 9d) at two different crack densities $e = 0.01$ and 0.05. The aspect ratio of the inclusions varies from $\alpha = 0.0001$ (flat cracks) up to $\alpha = 1$ (spheres). Figure 9 shows that the absolute values of δ, ε and γ are within the range 0–0.2, indicating that we are dealing with weak-to-moderate anisotropy (Thomsen 1986). These values increase for increasing crack density as might be expected. They all become zero for an aspect ratio $\alpha = 1$ (spherical inclusions), corresponding to an isotropic situation.

Note that for dry inclusions the values of δ, ε and γ have a non-zero constant value for a large range of aspect ratios and only go to zero for large aspect ratios.

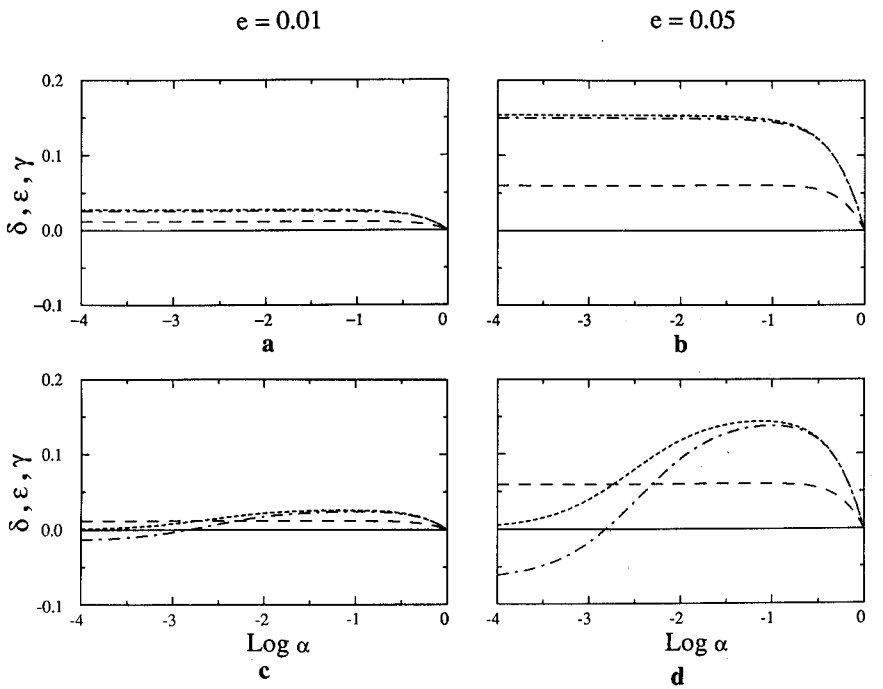

FIG. 9. The anisotropy parameters δ (·−·−·), ε (−−−−) and γ (———) calculated with Nishizawa's model as a function of the aspect ratio of dry (a and b) and liquid-filled inclusions (c and d). The results are shown for two crack densities $e = 0.01$ (a and c) and $e = 0.05$ (b and d).

Thus, for a large group of dry inclusions the resultant anisotropy is hardly affected by a change in aspect ratio. This conclusion corresponds to Fig. 3 which shows a very small variation in group velocities for small aspect ratios.

However, the liquid-filled inclusions show a large variation of the parameters δ and ε (Figs 9c and 9d) with the aspect ratio. Because both parameters are related to the qP- and qSP-wave velocities (see (1a) and (1b)) this variation corresponds to a strong dependence of the qP- and qSP-group velocity on the aspect ratio (as seen in Fig 2). Since the parameter γ (related to the qSR-wave) is constant for a large range of aspect ratios (especially for small aspect ratios), the group velocity of qSR-waves is not strongly affected by (small) aspect ratios (see Fig. 2).

For all the situations studied the values of ε and γ are positive, indicating that the phase velocities of the qP-and qSR-waves perpendicular to the axis of symmetry are always larger than those along this axis. For liquid-filled inclusions the value of ε goes to zero for very small aspect ratios, indicating that the difference between the qP-phase velocities in both directions also goes to zero.

Figure 2d shows this effect for the qP-group velocity at small aspect ratios. Figures 9a and 9b show this effect does not occur for dry inclusions where the parameter ε is non-zero for small aspect ratios.

Finally, Fig. 9 shows an interesting feature of the anisotropy caused by ellipsoidal inclusions, i.e. the parameters δ and ε are equal for aspect ratios $\alpha = 0.3$ up to $\alpha = 1$ for both liquid-filled and dry inclusions. This implies that the resultant anisotropy is elliptical, i.e. the qP- and qSR-wavefronts are ellipsoidal, while the qSP-wavefronts are spherical. Thus, we may conclude that media containing aligned ellipsoidal inclusions can be elliptically anisotropic.

Conclusions

This numerical study has shown that for a large range of aspect ratios of either liquid-filled or dry inclusions Crampin's and Nishizawa's models give similar results. Significant differences between the results exist only for large aspect ratios and crack densities (i.e. $\alpha > 0.3$ and $e = 0.05$).

Although Crampin's flat crack model is strictly valid only for small aspect ratios, it appears to model ellipsoidal inclusions with aspect ratios up to 0.3 reasonably well (considering a crack density $e = 0.05$). This implies that in the modelling of real data one may use Crampin's model even if the aspect ratios of the inclusions are not expected to be very small. For large aspect ratios and crack densities Nishizawa's model is more reliable and should be used. Otherwise Crampin's model is to be preferred because of its simple analytical form and the possibility of studying wave attenuation effects (due to scattering), which can not be done with Nishizawa's model.

For inclusions with large aspect ratios it is necessary to take the density of the effective medium into account. Otherwise the velocities modelled will be too low.

Finally, Thomsen's parameters δ, ε and γ prove to be useful for gaining a good impression of the anisotropy caused by all kinds of ellipsoidal inclusions. They show how inclusions with large aspect ratios result in elliptical anisotropy.

Acknowledgement

I thank K. Helbig for many discussions on the subject.

References

Alford, R.M. 1986. Shear data in the presence of azimuthal anisotropy: Dilley, Texas. 56th SEG Meeting, Houston, Expanded Abstracts, 476–479.

Anderson, D.L., Minster, B. and Cole, D. 1974. The effect of oriented cracks on seismic velocities. *Journal of Geophysical Research* **79**, 4011–4015.

Berryman, J.G. 1979. Long-wave elastic anisotropy in transversely isotropic media. *Geophysics* **44**, 896–917.

Crampin, S. 1978. Seismic wave propagation through a cracked solid: polarization as a possible dilatancy diagnostic. *Geophysical Journal of the Royal Astronomical Society* **53**, 467–496.

Crampin, S. 1981. A review of wave motion in anisotropic and cracked elastic-media. *Wave Motion* **3**, 343–391.

CRAMPIN, S. 1984. Effective anisotropic elastic constants for wave propagation through cracked solids. *Geophysical Journal of the Royal Astronomical Society* **76**, 135–145.

CRAMPIN, S. 1985. Evaluation of anisotropy by shear-wave splitting. *Geophysics* **50**, 142–152.

CRAMPIN, S. 1986. Anisotropy and transverse isotropy. *Geophysical Prospecting* **34**, 94–99.

CRAMPIN, S. 1987. Geological and industrial implications of extensive dilatancy anisotropy. *Nature* **328**, 491–496.

CRAMPIN, S., CHESNOKOV, E.M. and HIPKIN, R.G. 1984. Seismic anisotropy: the state of the art. *Geophysical Journal of the Royal Astronomical Society* **76**, 1–16.

CRAMPIN, S., EVANS, R. and ATKINSON, B.K. 1984. Earthquake prediction: a new physical basis. *Geophysical Journal of the Royal Astronomical Society* **76**, 147–156.

CRAMPIN, S., MCGONIGLE, R. and ANDO, M. 1986. Extensive-dilatancy anisotropy beneath Mount Hood, Oregon and the effect of aspect ratio on seismic velocities through aligned cracks. *Journal of Geophysical Research* **91**, 12703–12710.

CRAMPIN, S., MCGONIGLE, R. and BAMFORD, D. 1980. Estimating crack parameters from observations of P-wave velocity anisotropy. *Geophysics* **45**, 345–360.

DOUMA, J. and HELBIG, K. 1987. What can the polarization of shear waves tell us. *First Break* **5**, (3), 95–104.

ESHELBY, J.D. 1957. The determination of the elastic field of an ellipsoidal inclusion, and related problems. *Proceedings of the Royal Society, London*, Series A, **241**, 376–396.

GARBIN, H.D. and KNOPOFF, L. 1973. The compressional modulus of a material permeated by a random distribution of free circular cracks. *Quarterly Journal of Applied Mathematics* **30**, 453–464.

GARBIN, H.D. and KNOPOFF, L. 1975a. The shear modulus of a material permeated by a random distribution of free circular cracks. *Quarterly Journal of Applied Mathematics* **33**, 296–300.

GARBIN, H.D. and KNOPOFF, L. 1975b. Elastic moduli of a medium with liquid-filled cracks. *Quarterly Journal of Applied Mathematics* **33**, 301–303.

HELBIG, K. 1956. Die Ausbreitung elastischer Wellen in anisotropen Medien. *Geophysical Prospecting* **4**, 71–81.

HELBIG, K. 1958. Elastische Wellen in anisotropen Medien. *Gerlands Beiträge zur Geophysik* **67**, 177–211, 256–288.

HELBIG, K. 1979. Discussion on 'The reflection, refraction, and diffraction of waves in media with elliptical velocity dependence (F. K. Levin). *Geophysics* **44**, 987–990.

HELBIG, K. 1983. Elliptical anisotropy-its significance and meaning. *Geophysics* **48**, 825–832.

HELBIG, K. 1984. Transverse isotropy in exploration seismics. *Geophysical Journal of the Royal Astronomical Society* **76**, 79–88.

HOENIG, A. 1979. Elastic moduli of a non-randomly cracked body. *International Journal of Solids and Structures* **15**, 137–154.

HUDSON, J.A. 1980. Overall properties of a cracked solid. *Mathematical Proceedings of the Cambridge Philosophical Society* **88**, 371–384.

HUDSON, J.A. 1981. Wave speeds and attenuation of elastic waves in material containing cracks. *Geophysical Journal of the Royal Astronomical Society* **64**, 133–150.

KEITH, C.M. and CRAMPIN, S. 1977a. Seismic body waves in anisotropic media: reflection and refraction at a plane interface. *Geophysical Journal of the Royal Astronomical Society* **49**, 181–208.

KEITH, C.M. and CRAMPIN, S. 1977b. Seismic body waves in anisotropic media: propagation through a layer. *Geophysical Journal of the Royal Astronomical Society* **49**, 209–224.

KEITH, C.M. and CRAMPIN, S. 1977c. Seismic body waves in anisotropic media: synthetic seismograms. *Geophysical Journal of the Royal Astronomical Society* **49**, 225–243.

KREY, Th. and HELBIG, K. 1956. A theorem concerning anisotropy of stratified media and its significance for reflection seismics. *Geophysical Prospecting* **4**, 294–301.

NISHIZAWA, O. 1982. Seismic velocity anisotropy in a medium containing oriented cracks—transversely isotropic case. *Journal of Physics of the Earth* **30**, 331–347.

POSTMA, G.W. 1955. Wave propagation in a stratified medium. *Geophysics* **20**, 780–806.

RUDZKI, M.P. 1911. Parametrische Darstellung der elastischen Welle in anisotropen Medien. *Anzeiger der Akademie der Wissenschaften Krakau*, 503–536.

SCHOENBERG, M. and DOUMA, J. 1988. Elastic wave propagation in media with parallel fractures and aligned cracks. *Geophysical Prospecting* **36**, 571–590.

THOMSEN, L. 1986. Weak elastic anisotropy. *Geophysics* **51**, 1954–1966.

THOMSEN, L. 1988. Elastic anisotropy due to aligned cracks. *Geophysical Journal of the Royal Astronomical Society* (submitted).

UHRIG, L.F. and VAN MELLE, F.A. 1955. Velocity anisotropy in stratified media. *Geophysics* **20**, 774–779.

YALE, D.P. 1985. Recent advances in rock physics. *Geophysics* **50**, 2480–2491.